AFRL-HE-WP-TR-2002-0160

UNITED STATES AIR FORCE RESEARCH LABORATORY

Silver Colloids in Bacteria: A Study by Transmission Electron Microscopy, Absorption Spectroscopy And Elemental Analysis

B.V. Bronk
N. Faey
AFRL/HEST
Aberdeen Proving Ground MD 21010

M. Milan
R. Herd
Edgewood Chemical Biological Center
Aberdeen Proving Ground MD 21010

J. Czege
Z.Z. Li
Uniform Services University of the Health Sciences
Bethesda MD 20814

S. Efrima
Department of Chemistry and the Ilse Katz Center
For Meso- and Nano-Scale Science and Technology
Ben-Gurion University, Beer-Sheva, Israel

July 2002
Interim Report – Jun 1999 – September 2001

Human Effectiveness Directorate
Deployment and Sustainment Division
Operational Toxicology Branch
Chemical and Biological Defense Group
5183 Blackhawk Road
Aberdeen Proving Ground MD 21010-5424

When US Government drawings, specifications or other data are used for any purpose other than definitely related Government procurement operation, the Government thereby incurs no responsibility nor any obligation whatsoever, and the fact that the Government may have formulated, furnished, or in any way supplied the said drawings, specifications or other data, is not to be regarded by implication or otherwise, as in any manner licensing the holder or any other person or corporation, or conveying any rights or permission to manufacture, use, or sell any patented invention that may in any way be related thereto.

Please do not request copies of this report from the Air Force Research Laboratory. Additional copies may be purchased from:

National Technical Information Service
5285 Port Royal Road
Springfield, Virginia 22161

Federal Government agencies registered with the Defense Technical Information Center should direct requests for copies of this report to:

Defense Technical Information Center
8725 John J. Kingman Rd., Ste 0944
Ft. Belvoir, Virginia 22060-6218

TECHNICAL REVIEW AND APPROVAL

AFRL-HE-WP-TR-2002-0160

This report has been reviewed by the Office of Public Affairs (PA) and is releasable to the National Technical Information Service (NTIS). At NTIS, it will be available to the general public, including foreign nations.

This technical report has been reviewed and is approved for publication.

FOR THE DIRECTOR

STEPHEN R. CHANNEL, Lt Col, USAF, BSC
Director, AF CBD Tech Base Programs
Air Force Research Laboratory

REPORT DOCUMENTATION PAGE	Form Approved OMB No. 0704-0188

1. AGENCY USE ONLY *(Leave blank)*	2. REPORT DATE	3. REPORT TYPE AND DATES COVERED
	1 August 2002	Interim Report: June 1999 - September 2001

4. TITLE AND SUBTITLE

Silver Colloids in Bacteria: A Study by Transmission Electron Microscopy, Absorption Spectroscopy and Elemental Analysis

5. FUNDING NUMBERS

PE 62384B
PR 1400
TA 140001
WU 14000111

6. AUTHOR(S)

B.V. Bronk (1); N. Faey (1); Z.Z. Li (2); J. Czege (2); R. Herd (3); M. Milan (3); S. Efrima (4)

7. PERFORMING ORGANIZATION NAME(S) AND ADDRESS(ES)

(1) AFRL/HEST, Aberdeen Proving Ground MD; (2) Uniform Services University of the Health Sciences, Bethesda MD; (3) Edgewood Chemical Biological Center, Aberdeen Proving Ground MD; (4) Department of Chemistry and the Ilse Katz Center for Meso- and Nano-Scale Science and Technology, Ben-Gurion University, Beer-Sheva, Israel

8. PERFORMING ORGANIZATION REPORT NUMBER

9. SPONSORING/MONITORING AGENCY NAME(S) AND ADDRESS(ES)

Air Force Research Laboratory, Human Effectiveness Directorate,
Deployment and Sustainment Division, Operational Toxicology Branch,
Chemical and Biological Defense Group
E5183 Blackhawk Road
Aberdeen Proving Ground MD 21010-5424

10. SPONSORING/MONITORING AGENCY REPORT NUMBER

AFRL-HE-WP-TR-2002-0160

11. SUPPLEMENTARY NOTES

12a. DISTRIBUTION AVAILABILITY STATEMENT

Approved for public release; distribution is unlimited.

12b. DISTRIBUTION CODE

13. ABSTRACT *(Maximum 200 words)*

Reduction of silver ions in and on bacterial cells was shown to produce silver colloids giving rise to intense surface enhanced Raman spectra (SERS) of chemical components of the cell. Transmission electron microscopy, absorption spectroscopy and elemental analysis were used to explore the distribution of silver in and on the cells produced by two different protocols. The first protocol gives rise to an internal colloid of nanometer sized silver particles uniformly distributed within the cells. The second protocol produces a rough (aggregated) silver layer on the cells surface. Both protocols largely preserve the shape of the cells although there is a size reduction, which is to be detailed in a subsequent report. Treatment with Potassium cyanide removes the silver and reverts the cells to a size and shape similar to the original.

14. SUBJECT TERMS

Silver Colloids and Bacteria; SERS and Bacteria; Colloids Formed with Bacteria

15. NUMBER OF PAGES

16. PRICE CODE

17. SECURITY CLASSIFICATION OF REPORT	18. SECURITY CLASSIFICATION OF THIS PAGE	19. SECURITY CLASSIFICATION OF ABSTRACT	20. LIMITATION OF ABSTRACT
Unclassified	Unclassified	Unclassified	SAR

THIS PAGE INTENTIONALLY LEFT BLANK

TABLE OF CONTENTS

Page

Summary 1

Introduction 1

Experimental 2

Bacteria, Growth Conditions, and Chemical Preparation 2

Results and Analysis – Electron Microscopy 3
Internal Colloid 3
Wall Coating 12
UV-visible Absorbance Spectroscopy 14
Elemental Analysis 17

Discussion and Conclusions 18

References 20

FIGURES

Figure Page

1. *Escherichia coli* cells with internal silver colloid. Magnification 3400x 4
2. Enlargement of section of Figure 1. Magnification 13,200x. Note that one cell has broken releasing most of the silver particles. The line across the diameter indicates where intensities are measured for Figure 3. 4
3. Log of relative intensity for indicated cell in Fig. 2 is plotted against position across the silver treated *E. coli's* rodlike short diameter. The solid curved line is the fit to experiment according to equation (1). In this figure, larger numbers indicate lighter pixels 6
4. Electron micrograph of a control cell of *E. coli*. Magnification 24,500x. This cell was treated with borohydride only, but no silver nitrate. Controls with no chemical treatment, but only washes were similar in size and appearance 7
5. A silver treated cell shown after CN^- treatment removed the silver. Magnification 24,500x 8
6. Log of relative intensity of CN^- treated cell of Fig. 5 plotted vs position across the short diameter 8
7. Silver treated *E. coli* cells after heavy CN^- treatment removes all silver 9
8. *Bacillus megaterrium* cells infused with silver by the direct protocol. Magnification 6200x 10
9. Calculated and measured ln intensity curves vs position, for the silver infused *Bacillus* cell indicated in Fig. 8. The cell radius is 115 pixels. $\varepsilon^*=2.3\varepsilon$ X δ, with ε the molar extinction coefficient of silver for electron-atom scattering, C the silver atom concentration in the cell, and δ is the pixel scale (230 pixels are ~1μm) $\varepsilon^* = 0.0085$ so $\varepsilon = \sim 8 \times 10^4 cm^{-1}M^{-1}$, that is the same order of magnitude as we found for *E. coli* 10
10. SERS spectra obtained from Gram-negative and a Gram-positive bacteria in separate preparations with the Wall Coat protocol 11
11. *Bacillus megaterrium* cells infused with unreduced silver ions. Magnification 13,400 12
12. *Escherichia coli* cells with the Wall Coat (reverse) protocol forming silver on the exterior. Magnification 6200x 12
13. Log of relative intensity for a Wall Coated *E. coli* cell plotted against position across the silver coated cell's rodlike short diameter 14
14. UV- visible absorption spectrum of suspension of *E. coli* cells with Internal Colloid (non filtered). Inset is spectrum of filtrate passed thru a 0.22 μm filter which excludes the bacteria 15
15. UV vis. absorption of a suspension of *B. meg* cells, after direct protocol showing spectrum of an internal silver colloid 16
16. UV-vis absorption of a suspension of *E. coli* cells after the reverse protocol produced wall coated cells 16
17. UV-vis absorption of a filtered colloidal suspension of silver nanoparticles obtained after treating a solution of Yeast extract with silver ions followed by reduction with sodium borohydride. Essentially the same spectrum but ~10% more intense was obtained from the unfiltered suspension 17

TABLES

Table Page

1. Results of Elemental Analysis..... 18

Summary:

Raman spectra are known to produce characteristic and unique fingerprints for individual chemicals. Thus there is some prospect for using these spectra for identifying or classifying suspected bacterial agents through their chemical differences. The major obstacle to this is the weak Raman signal arising from trace chemicals. In the future this may be overcome by use of Surface Enhanced Raman spectra (SERS) which can increase a signal by several orders of magnitude. Reduction of silver ions in and on bacterial cells was shown to produce silver colloids giving rise to intense SERS of chemical components of the cell. Transmission electron microscopy, absorption spectroscopy and elemental analysis were used to explore the distribution of silver in and on the cells produced by two different protocols. The first protocol gives rise to an internal colloid of nanometer sized silver particles uniformly distributed within the cells. The second protocol produces a rough (aggregated) silver layer on the cells surface. Both protocols largely preserve the shape of the cells although there is a size reduction, which is to be detailed in a subsequent report. Treatment with Potassium cyanide removes the silver and reverts the cells to a size and shape similar to the original. This is basic research which is expected to improve the understanding of SERS spectra (and thus the related IR spectra) arising from bacteria. This knowledge will facilitate development of instrumentation for rapid classification of suspected biological agents.

Introduction

Bacterial cells can serve as a particularly interesting and relatively unexplored environment for the production of colloids. They impose limitations on the availability of the precursors and their motion, and, more importantly, they offer a variety of chemical sites that can alter the course of the particle-generating reactions. Thus, bacteria can affect the particle size distribution, as well as the stabilization of the colloid, both of which are important issues for materials science and the physical chemistry of particulate systems. On the other hand, the production of colloids in association with bacteria can be useful for the study of bacteria and their structural features, as well as for understanding phenomena such as biomineralization, and for applications such as developing technologies of chemical waste bio-treatment. It was recently shown that high intensity surface enhanced Raman spectra (SERS) were exhibited by bacteria infused with silver colloids [Reference 1,2]. Two major protocols were adopted where the colloid was formed either primarily inside the bacterial cell (*Internal Colloid*), or produced a rough metal coating on its external wall (*Wall Coat*). In the latter case the main features in the intense Raman spectra are attributed to flavin containing constituents of the bacteria wall [Reference 3]. (Examples of such spectra are shown in the Results section.) The weaker spectrum from bacteria with an *Internal Colloid* is not yet assigned. The present study concentrates on other available techniques to elucidate the association of the inorganic colloids and the bacterial components in order to further the utility of present and future Raman studies.

Recent studies [Reference 4-6] showed that silver colloids produced by *Pseudomonas stutzeri* accumulate as large faceted granules within the bacterial cell. Some earlier studies of interest considered mineral accumulation in mostly natural (even though they might be polluted) circumstances[Reference 7-10]. In contradistinction, we consider here the introduction of (silver) particles into bacteria by artificial means, by "test-tube like" solution chemistry.

In this report we consider the spatial distribution of silver metal in the bacterial cell, prepared by the *insitu* reduction of silver ions with sodium borohydride. We focus here on the corresponding changes in the cells, based on transmission electron microscopy (TEM), UV-visible extinction spectroscopy, and elemental analysis. Further studies based on light scattering and TEM measurements of cell size decrements associated with the chemical protocols are to be presented in a subsequent report. As SERS is associated with molecules in immediate proximity of the silver particles, their position within the microorganism is of prime importance when one sets out to interpret the Raman spectra in terms of a specific biochemical environment. In addition, it is important to know where the silver tends to accumulate under a variety of circumstances, when one wishes to place it in designated areas within the bacteria, to achieve specificity. Finally, one would want to know what changes occur in the bacterial system, following the chemical treatment we use to introduce the metal colloids. This is of interest especially when one aims to use this colloid-induced SERS as a tool to study the biochemistry of the bacterial cell as well as changes in the cell's chemistry with time, or under a variety of external stresses and stimuli.

Experimental

Bacteria, Growth Conditions, and Chemical Preparation

Two species of bacteria were used in the experiments discussed here, one gram negative, *Escherichia coli* (ATCC 49539, American Type Culture Collection, Rockville, MD), and one gram-positive species, *Bacillus megaterium* (ATCC13632, a non-sporulating strain).

Both species were grown under well-aerated conditions in a reciprocating shaker at 32 °C (*E. coli*) or 37 °C (*B. meg.*). The growth medium used is LB (ATCC medium 1065) formulated as 10.0 g NaCl, 10.0g tryptone and 5.0 g yeast extract (Difco 0127) per liter distilled water. A specific stage of growth was chosen in order to provide uniform populations of cells.

Cells were grown from a slant overnight and then re-inoculated into fresh medium. Growth was then followed by Optical density (OD) measurements at 600 nm until the logarithmic growth curve appeared to be near maximum curvature (minimum second derivative) in its approach to stationary phase. The OD here was 0.6-0.8 for *E. coli* or 0.5-0.7 for *B. meg*, at which point cells were harvested. To eliminate chlorides and avoid precipitation of silver chloride, the bacteria were washed twice (i.e., three centrifugations, typically at ~2400 g's for 10 min at 10 °C). After each centrifugation, the supernatant was discarded, and the cells were resuspended in distilled, deionized water. At this point, cells were often treated with formaldehyde (at the very low 0.1% final concentration for twenty minutes) in order to preserve the shape of the cells for transmission electron microscopy (TEM). Compared to treatments which omitted this step there was no noticeable change to the size or shape of the cells as indicated by TEM and light scattering, nor were the Raman results affected from this very low concentration of formaldehyde. This very mild treatment did prevent distortion of the shape of control cells as observed by TEM (without the treatment, some bending of the rod ends of control cells was observed).

After this treatment, the cells were centrifuged and the supernatant discarded, following which one of the following two procedures was carried out, using silver nitrate and sodium borohydride from Aldrich.

In the *Internal Colloid* or direct procedure, the bacteria were suspended in a 0.05 M silver nitrate aqueous solution. The suspension was allowed to sit for 20 minutes and then washed twice with distilled water as above, and finally resuspended in a 0.1 M solution of sodium borohydride. It

was then washed again twice with distilled water and centrifuged to concentrate the cells as appropriate for microscopy or polarized light scattering (or SERS measurements).

In the *Wall Coat* or reverse procedure, the cells were suspended in 0.1M sodium borohydride. The cells were centrifuged and the supernatant discarded to get rid of excess borohydride. The cells were immediately resuspended in a silver nitrate solution at concentrations of either .05M or 5 x 10^{-4} M. The reductant remaining in the cells diffuses out to meet the silver ions diffusing in and a deposit apparently forms primarily at the wall where the two fronts meet.

A standard procedure to remove silver from the treated cells, was to dilute some stock solution of 0.1 M KCN into a distilled water suspension of the cells for a final concentration of 1 mM of CN^-. Within 10 min the silver would dissolve and then light scattering or TEM experiments would be performed. Lower concentrations of cyanide were sometimes used for partial removal of the silver.

A Phillips C100 microscope was used for transmission electron microscopy (TEM) with an ~80 KV accelerating voltage. The TEM micrographs shown here are made without any of the usual preparations for enhancing the image. The procedure only utilized the silver used in the preparations described above, and/or the very low concentration formaldehyde fixation described to maintain the shape of cells which had no silver (controls) or had the silver removed (cyanide treated). Formaldehyde is not mandatory, the same results were obtained without it, except that it proved helpful in eliminating or reducing shape distortion from TEM images for the controls. Ten μL of a suspension containing the cells were deposited onto Lacy Formvar/carbon-coated copper grids (Pelco International 01882-F 300 mesh grids). At times polystyrene microspheres of size 0.993 ±0.021 micrometers (Duke Scientific, Cat #4009A) were added to the cell suspension prior to layering on the grids to provide a calibration standard for the micrographs.

UV-visible absorption spectra were taken with a Beckman Model DU 7400 diode array using matched quartz cells with a 1 cm pathlength.

During many of the preparations, we separated an aliquot of the silvered and/or control cells in distilled deionized water for elemental analysis. The total organic carbon (TOC) was measured with a Durham DC-80 TOC system. The silver content was measured for the same cells after acidifying with ~ 2% nitric acid. For this we used a Perkin-Elmer Plasma II Inductively Coupled Plasma system.

Results and Analysis

Electron Microscopy

Internal Colloid

Figure 1 shows the main features we observe for *E. coli* bacteria treated in the direct protocol, designed to produce a silver colloid uniformly dispersed within the entire bacterial cell. The sample contains mostly cells that appear intact, with a few obviously damaged cells. The intact, smooth, dark bacteria, are typically ~ 2-3 μm long and~0.9 μm wide. The smooth outer shape of the cell suggests that the silver is mostly contained within it rather than aggregating on the surface.

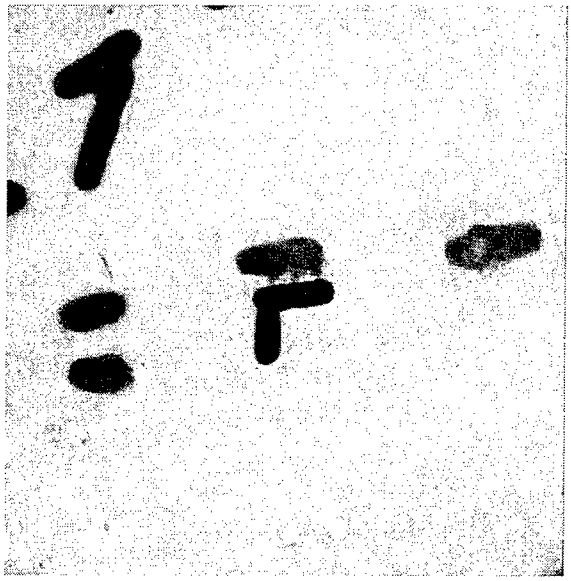

Figure1. *Escherichia coli* cells with internal silver colloid. Magnification 3400x.

A few of the cells of Figure 1 (center) are shown enlarged in Figure 2 in a gray scale scheme, where one can see that the grayscale intensity increases (i.e., becomes darker) gradually as the cell's center is approached across the marked section.

Figure 2. Enlargement of section of Figure 1. Magnification 13,200x. Note that one cell has broken releasing most of the silver particles. The line across the diameter indicates where intensities are measured for Figure 3.

Under typical conditions, *Escherichia coli* cells are seen as spherically capped cylinders when viewed with no special treatment either under a phase-contrast microscope or with TEM here and have been successfully modeled as such to fit light scattering data [Reference 11]. With the assumptions of such a cylindrical shape, a uniform distribution of silver within such a cylinder, and the further assumption that the scattering of the electrons in the TEM is proportional to the local concentration of silver (electrons) and that the darkening of the image is linearly related to the intensity of the transmitted portion of the electron beam a quantitative analysis based on the Beer-Lambert law is made below:

Let the transmitted intensity at a distance x from the cell wall, along a line cut through the bacterium (see Figure 2) be $I_1(x)$. $I_1(0)$ is the intensity just outside the cell (thus correcting for the background). Assuming that the cell retains its cylindrical shape with cross-section radius R we get

$$(1) \qquad I_1(x) = I_1(0)\exp\{-2*2.3\varepsilon C[R^2-(x-R)^2]^{1/2}\}$$

$$= I_1(0)\exp\{-2.3\varepsilon^*[N_R^2-(N_x - N_R)^2]^{1/2}\}$$

with $x \in [0,2R]$ inside the cell, and converting to pixels, with N_x being the number of pixels corresponding to the radius of the cell and the position x within it, respectively, in Figure 2. Our calibration of the micrograph indicated 222 pixels ~1 μm giving the size of one pixel, δ as 4.5 nm and the number of pixels for R~ 1/2 μm is then N_R= 111. A factor 2 is provided to account for the full cylindrical chord at position x. The fit uses one free parameter, $\varepsilon^*=2\varepsilon C\delta$, with ε being the molar extinction coefficient of silver for electron-atom scattering, C is the silver atom molar concentration in the cell, and δ is the physical size on the grid corresponding to a pixel in Figure 2.

A fit of this theoretical prediction to the measured intensity of the TEM image across the bacterial cell is shown in Figure 3. The reasonable agreement between the shapes of the measured and predicted functions suggests that indeed the cells generally retain their approximately cylindrical shape. This conclusion is corroborated by several other observations. First, similar analyses of other preparations (cyanide treated cells, Figure 5, silver-infused *B. meg* cells, Figure 8 and reverse (Wall Coat) treated bacteria, Figure 11) yield a consistent behavior (see below). Second, the general cell shape is retained in the intact bacteria in Figure 2. Third, a comparison to the micrograph of the damaged cell in Figure 2 that appear to be flatter agrees with this conclusion. This conclusion is supported also by a comparison to the TEM of the cells shown later (Figures. 5 and 7) exhibiting empty and flattened shells.

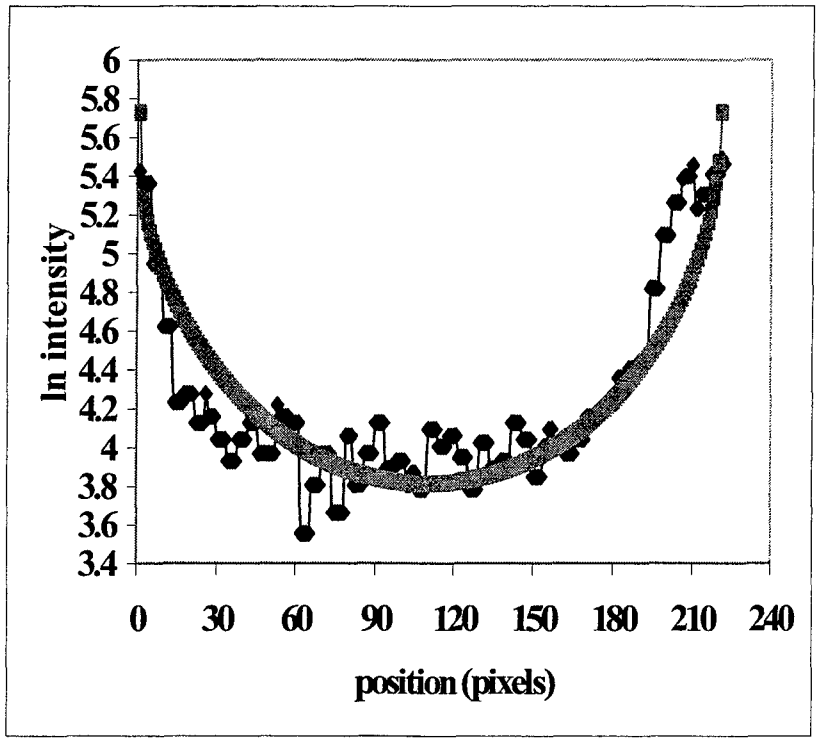

Figure 3. Log of relative intensity for indicated cell in Fig. 2 is plotted against position across the silver treated *E. coli's* rodlike short diameter. The solid curved line is the fit to experiment according to equation (1). In this figure, larger numbers indicate lighter pixels.

We find from the fit ε^* ~0.0075. As shown later, on the basis of elemental analysis, the estimated concentration of the silver atoms in the cell for this preparation protocol is 0.2-0.3M, yielding a molar extinction coefficient of ~ε=3-4 x10^4 $cm^{-1}M^{-1}$. This is equivalent to a decay reciprocal length of 0.6-0.9nm^{-1} for solid silver ε*C=4x10^4*1000*10.5*2.3/108=9x10^6 cm^{-1} =0.9nm^{-1}. The corresponding decay distance of ~ 1 nm compares favorably with electron mean free path of metals ~1-5nm [Reference 12].

The obviously damaged bacterial cells in Figure 1 probably broke apart during the preparation of the TEM samples or the application of the vacuum. The colloidal content in the form of black particles seen to be spewed out nearby (e.g., Figure 2) is consistent with this description. In parallel, the gray-scale intensity (i. e. the silver content) of the damaged bacterium itself decreases (typically by 1/3) compared to an undamaged cell, especially near the rupture. The particles surrounding the damaged cell are typically 5-10 pixels in diameter, i.e. 22—45 nm. Previously [Reference 1], we found that ~2nm colloidal particles are formed when prepared in *E. coli* bacteria using our procedure, and also 4-10 nm silver particle aggregates are often observed in our TEM micrographs. Thus, Figure2 again strongly suggests that the colloidal particles are initially dispersed homogeneously within a fluid phase throughout the bacteria. Once the cell-wall breaks, they flow out with the cell contents and may partially aggregate. Note also that the damaged cells appear flattened, especially near the rupture, giving further credence to our assumption that the undamaged silver-treated cells retain their cylindrical form. The ability to break the cells and to harvest the colloids may be interesting for applications in colloid science.

The *E. coli* controls which are not treated to produce silver particles look very different from the treated ones (See Figure 4). The contrast is much lower, and the larger intensity along the "bacterial rod's" center line, probably reflects the larger width along the major axis of the initially cylindrical cell. These observations are in keeping with the known rod-like shape of the bacteria. There are also decreases in the size of silver treated cells, which we expect to discuss in a subsequent report.

Figure 4. Electron micrograph of a control cell of *E. coli*. Magnification 24,500x.
This cell was treated with borohydride only, but no silver nitrate. Controls with no chemical treatment, but only washes were similar in size and appearance.

Another treatment was used to further elucidate the effect of the silver on the bacterial cells. In this case after bacteria were subjected to the full silver and reductant stages (including washing and centrifugation), potassium cyanide was added to remove the silver. In the presence of oxygen the cyanide induces a fast oxidation of the silver metal to silver ions. The ions then may slowly diffuse out of the damaged cell.

An example is shown in Figure 5. The TEM micrographs become much brighter and the bacteria show dark and light patches not necessarily located along the "backbone" of the cell which could indicate shape distortion or some remaining silver. The bacteria appear somewhat deformed from the original cylindrical shape, and there are often many more obviously flattened cells (See also Figure 7).

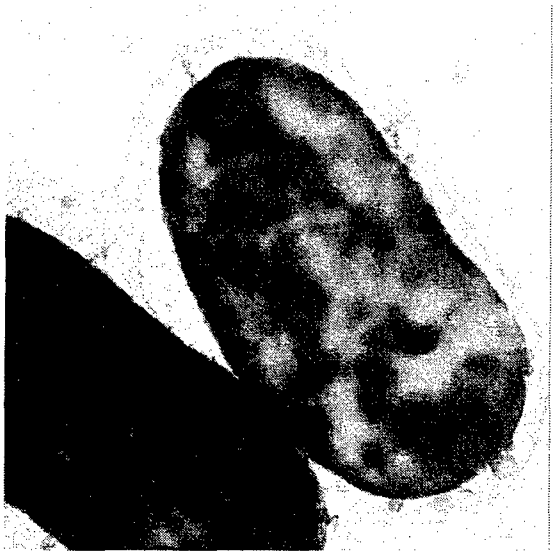

Figure 5. A silver treated cell shown after CN^- treatment removed the silver. Magnification 24,500x.

The density profile observed for treated cells after the silver is removed, is significantly different than that observed for the colloid-containing cells. A typical profile is shown in Figure 6. There is no indication of increasing attenuation of the electron beam as the central ridge of the bacterium is approached, as previously seen in Figure 3. The over all shape of the bacteria remains similar to that of the control cells though their aspect ratio becomes smaller, and is smaller compared to the colloid-containing cells.

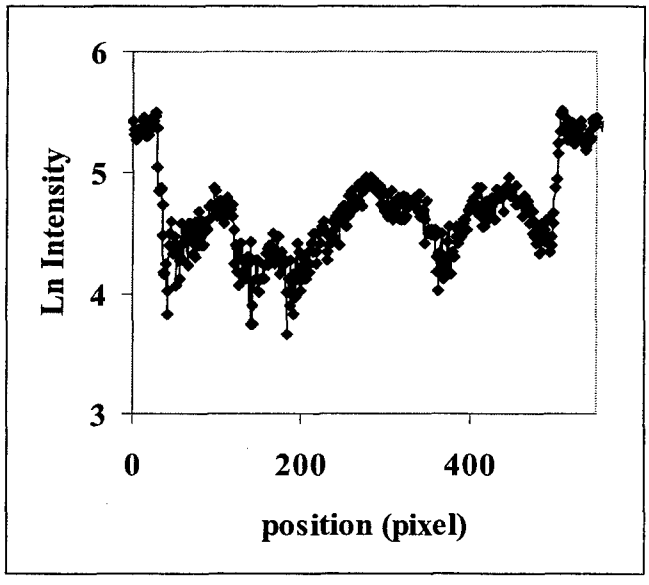

Figure 6. Log of relative intensity of CN^- treated cell of Fig. 5 plotted vs position across the short diameter.

Under a more aggressive treatment with cyanide (higher concentration) the bacteria lose all their silver and become somewhat bloated and almost transparent as seen in Figure 7, yet retaining to some extent the general shape of the control cells. The treatment with cyanide invariably causes a swelling of the silvered cells. However, the cells appear similar in shape to the control cells suggesting that the cell wall is largely intact also at the previous stage, when the colloid infuses the cell. The dimensions continue to increase toward those of the control cells with a concomitant decrease of aspect ratio, as the concentration of the cyanide increases. At times, the cyanide treatment at high concentration is destructive to the integrity of the cells so that some of them lose all their contents, and only the wall-shells remain and are observed lying flat on the grid. Mildly fixing the bacteria with 0.1% formaldehyde prior to the silver and reduction stages does not make any noticeable difference in the dimensions of the intact cells under the treatment described above. For brevity we do not reproduce the micrographs here.

Figure 7. Silver treated *E. coli* cells after heavy CN^- treatment removes all silver.

Bacillus megaterrium is another species of bacteria which was investigated. In contrast to the Gram-negative *E. coli*, these bacteria are Gram-positive and are much larger. The control, native cells of *B. meg* are ~4.5--8 μm long by ~1.5 μm in diameter.

In the direct protocol (silver followed by reduction), except for a capsule which does not stain, the bacteria appear to the eye rather uniformly dark as may be seen in Figure 8. However the intensity histogram in Figure 9 shows a gradual intensification across the cylindrical diameter, as seen above with *E. coli*. The analysis shown in that Figure again gives a good fit based on Beer-Lambert extinction for a cylindrical object lying on its side. We obtained an extinction coefficient of ~1.6×10^4 $cm^{-1} M^{-1}$, the same order of magnitude found for *E. coli*, giving an electron mean free path in silver of 3 nm. An approximately uniform distribution of the silver within these Gram-positive bacterial cells is confirmed by the excellent fit of the calculation to the experimentally measured attenuation of the electron beam shown in Figure 9.

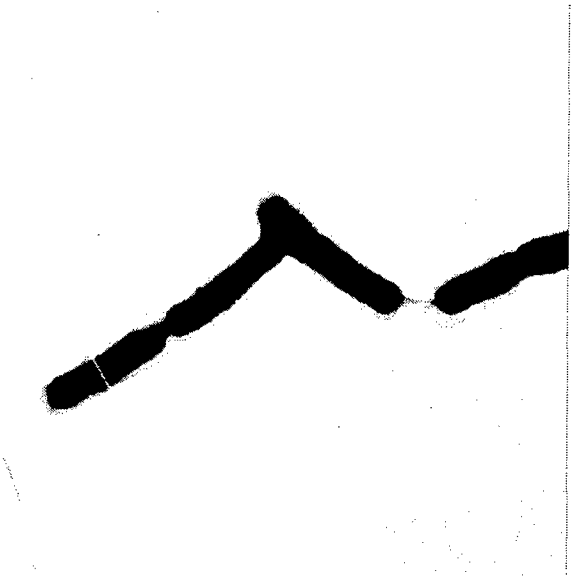

Figure 8. *Bacillus megaterrium* cells infused with silver by the direct protocol. Magnification 6200x.

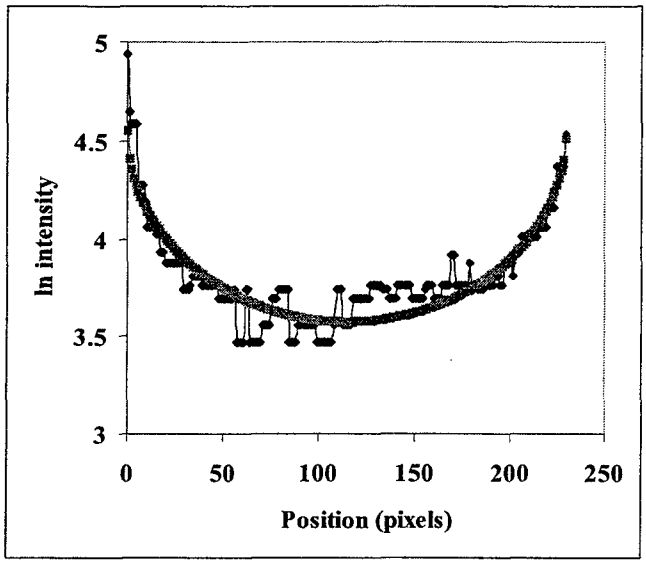

Figure 9. Calculated and measured ln intensity curves vs position, for the silver infused *Bacillus* cell indicated in Fig. 8. The cell radius is 115 pixels. $\varepsilon^*=2.3\varepsilon$ X δ, with ε the molar extinction coefficient of silver for electron-atom scattering, C the silver atom concentration in the cell, and δ is the pixel scale (230 pixels are ~1μm) $\varepsilon^* = 0.0085$ so $\varepsilon = \sim 8 \times 10^4 cm^{-1}M^{-1}$, that is the same order of magnitude as we found for *E. coli.*

Excellent SERS spectra were also successfully produced from this species using the same preparations described here. Examples of a *B. meg* spectrum and an *E. coli* spectrum, both obtained with the Wall Coat protocol, are compared in Figure 10. Further experiments are required to determine whether any of the differences in such spectra for the two species are

significant. The main features of both of these spectra are attributed to flavins contained in the cell wall/membrane[Reference 3].

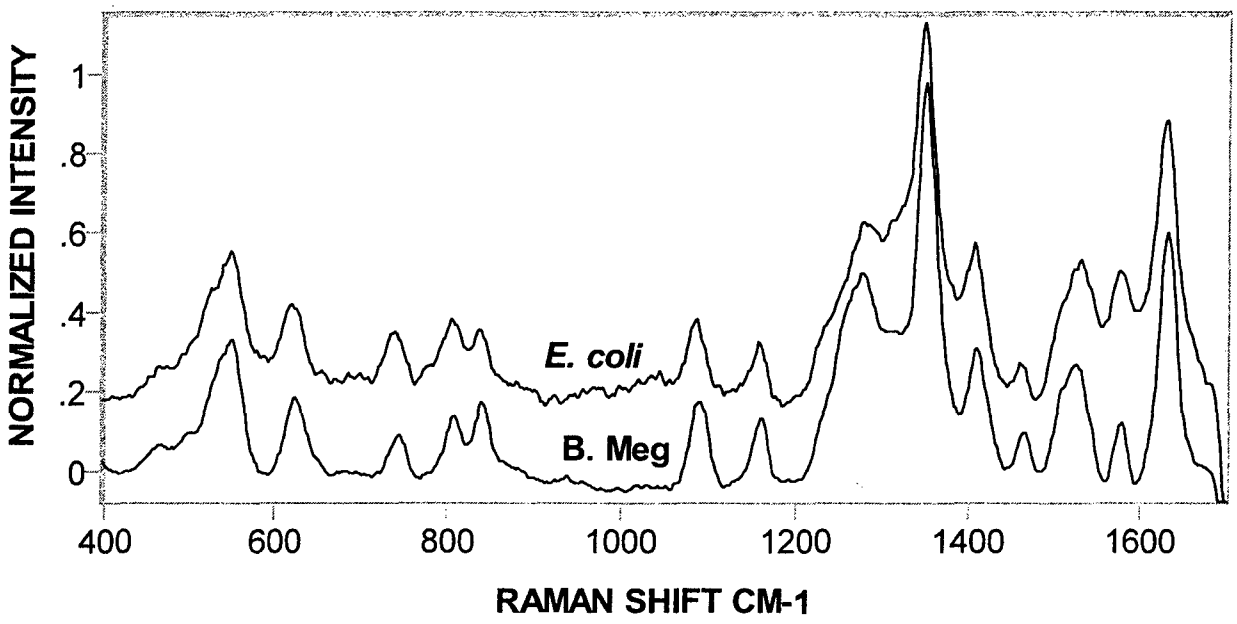

Figure 10. SERS spectra obtained from Gram-negative and a Gram-positive bacteria in separate preparations with the Wall Coat protocol.

Because of the complex treatment protocols, several different controls were run at various times for *E. coli* as well as for *B. meg* cells. (i.e., no chemical; borohydride only; silver ions only with no borohydride.) The reduction in cell dimensionsdue to silver coating mentioned elsewhere were not observed for any of these controls.

Figure 11 shows a micrograph of *B. meg* cells with silver ions but no silver particles. Again, the electron dense region appears uniform throughout the cell, and shows a sharp edge. It is notable that there is an electron dense region in the neck between just divided *B. meg* cells which sometimes showed up with the reduction step (silver particles) also with these cells but not for *E. coli* cells.

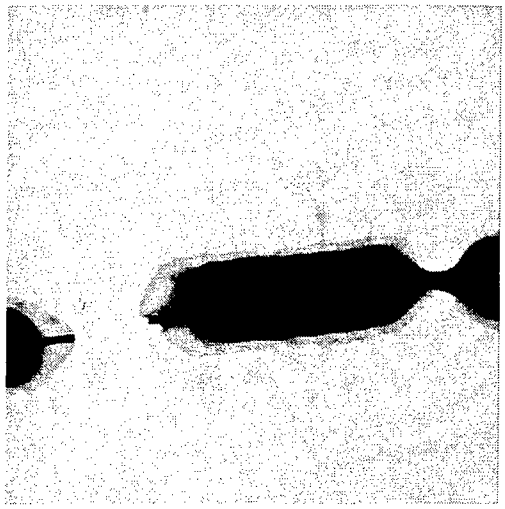

Figure 11. *Bacillus megaterrium* cells infused with unreduced silver ions. Magnification 13,400.

Wall Coating

We now return to *E. coli* and discuss the results obtained, when the order of the introduction of silver nitrate and the reductant is reversed, so that a wall coat is formed. In this case the bacteria shown in Figure 12 evidently have somewhat rough exteriors, with aggregates of dark matter, probably silver colloidal particles, adhering to them. The general outline of the cells is still observed, indicating a coating that is still much thinner than the dimension of the cell itself, probably <~1/10 of the cell waist, i. e. < ~100 nm; see below). In comparison to silver ions, sodium borohydride appears to have a much weaker affinity to the cell; since after long washes we observed no silver reduction (i.e.,apparently essentially all the reductant is removed). However, sufficient amounts remain following a brief and rapid wash sequence, to chemically reduce incoming silver ions and form a coat of silver around the cell as seen in Figure 12.

Figure 12. *Escherichia coli* cells with the Wall Coat (reverse) protocol forming silver on the exterior. Magnification 6200x.

One can estimate a maximum of the average thickness of the silver deposit, assuming that all the sodium borohydride is retained in the cell even after the short washes, and that all of it is utilized to reduce silver ions. With an initial ambient molar concentration of $NaBH_4$, C (=0.1M=1x10^{-4} mol/cc), a cylindrical cell waist radius of R_{cell} (=0.75μm), and assuming equipartitioning of $NaBH_4$ between the aqueous solution and the cell, the thickness, d, of the silver coat on *E. coli* would be

$$(2) \qquad d=4(M_{Ag+}/\rho_{Ag+})\, CR_{cell} \sim 4x10^{-3}\, R_{cell}=3nm$$

M_{Ag+} is the atomic mass of silver, ρ_{Ag+} is its density (=10.5g/cc), and we take 8 electrons per molecule of borohydride used for reduction of silver. This is the maximum value one would expect for the average thickness of the shell. The TEM micrographs suggest that the thickness might be larger than that, indicating the presence of larger amounts of the reductant than expected on the basis of the size of the cell. Thus, the brief washes might leave some of the reductant in the solution that remains adhered to the cells or that fills the gaps between them in the pellet after centrifugation. Indeed when applying longer washes (5-10 min) only small amounts of colloid form, insufficient for producing measurable SERS. The presence of the reductant near the wall, and a possible catalytic function of the wall may be the reason why the reduction of the silver ions occurs mainly on the cell wall, producing the silver coat, rather than a colloid inside the cell.

The silver-coated cells tend to adhere to each other, forming cell aggregates (Figure 12), as can be seen also from the texture of the treated bacteria. This is consistent with the strong attraction expected between the silvered cells (with a large Hamaker constant) and their irreversible aggregation. Often clumps of loose particles are also seen to adhere to the cells. An intensity line profile (in a log scale) across a typical silvered-coated cell is shown in Figure 13. Here the picture obtained corresponds to an abrupt increase of electron density, which remains constant across the cell rather then the gradual change implied by the histogram in Figure 3 for cells infused with an internal colloid. This gives further support to the conclusion that large quantities of silver are concentrated mainly on the external wall of the bacteria. The metal shells are sufficiently thick to prevent significant penetration through the cells by the electron beam.

On the basis of the transmitted beam intensity we measured for the internal silver colloid (see discussion following eq. 1), and the known silver concentration in the cell in that case (0.2-0.3M), we can estimate the minimum silver coat thickness expected to give rise to the opacity seen in Figure 13. We find it to be at least 1-2nm, taking into account that the beam needs pass twice through the silver coat. This is in line with our previous estimate, though we cannot yet determine the precise thickness within the range 2-100 nm from these data alone. The strong SERS signals we observe (see Figure 10) indicate that the silver film most probably cannot be thicker than 10-20nm, as otherwise it would not be sufficiently transparent to allow for the strong SERS. From our examination of the size changes of the cells, we estimated a similar coat thickness which we expect to discuss in a subsequent report. Thus we find an average silver coat which is probably no more than a few nm thick. Using electron microscopy of cell sections we hope to be able to confirm these values of the shell thickness, in a future stage of the research.

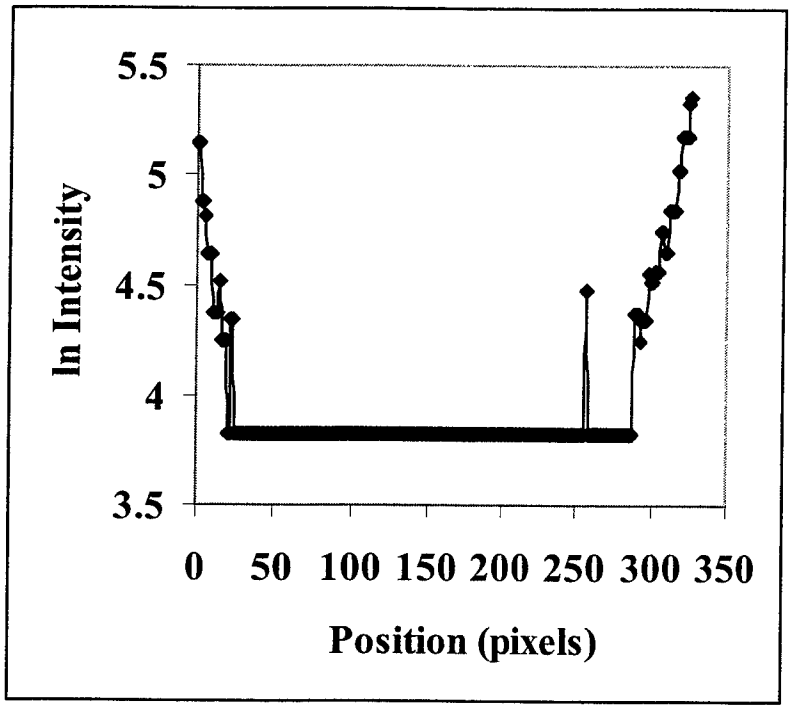

Figure 13. Log of relative intensity for a Wall Coated *E. coli* cell plotted against position across the silver coated cell's rodlike short diameter.

Our findings described above do not exclude the possibility of the presence of the silver inside the cell when the "reverse" protocol is used. We believe, however, that this is minimal. The propagating diffusional fronts of the silver ions (coming from the ambient solution) and that of the borohydride moving rapidly across the submicron distance from the interior of the cell towards its exterior, or already located in the fluid outside but near the individual cells, meet at the bacteria wall. As they meet there, a silver deposit forms, that would tend to act as a physical barrier for significant penetration of silver ions into the cell. Furthermore, the silver deposit at the wall will serve as an efficient nucleation center for all additional deposition to occur predominately there.

As was seen for an internal colloid, treating the wall coating with cyanide dissolves away most of the silver and the cells swell up, retaining an elongated ovoid shape with some resemblance to the control cells. For brevity we do not show the micrographs here. Although the chemical treatments cause some disruption of the cell wall, as evidenced by the swelling of CN^- treated cells compared to untreated control cells, the cell-wall for many of the cells must remain largely intact to preserve the elongated shape.

UV-visible absorbance spectroscopy

Figure14 shows the UV-visible absorption spectrum of a suspension of *E. coli* bacteria with an internal colloid, and the insert to that Figure shows the spectrum of the filtrate obtained after filtering the suspension through a 0.22 μm filter. The well-defined maximum of the extinction at 400nm is a clear signature of a silver colloid composed of individual, non-aggregated nanoparticles. The absence of the colloid spectral feature in the filtrate once more confirms that

the particles are largely associated with the bacteria. However, the filtrates are not always as clean as the one shown here. Some do show a clear indication of the presence of colloids. These probably are released into solution from damaged bacteria (e.g., See the TEM micrograph of Figure1). It is improbable that they formed directly in solution to any large extent, as the concentration of silver ions there at the reduction stage, is extremely low. Thus, the UV-vis spectra support the conclusion that in the "Internal Colloid" the silver is dispersed through out the bacterial cell as individual, small (~3nm [1]) separate particles.

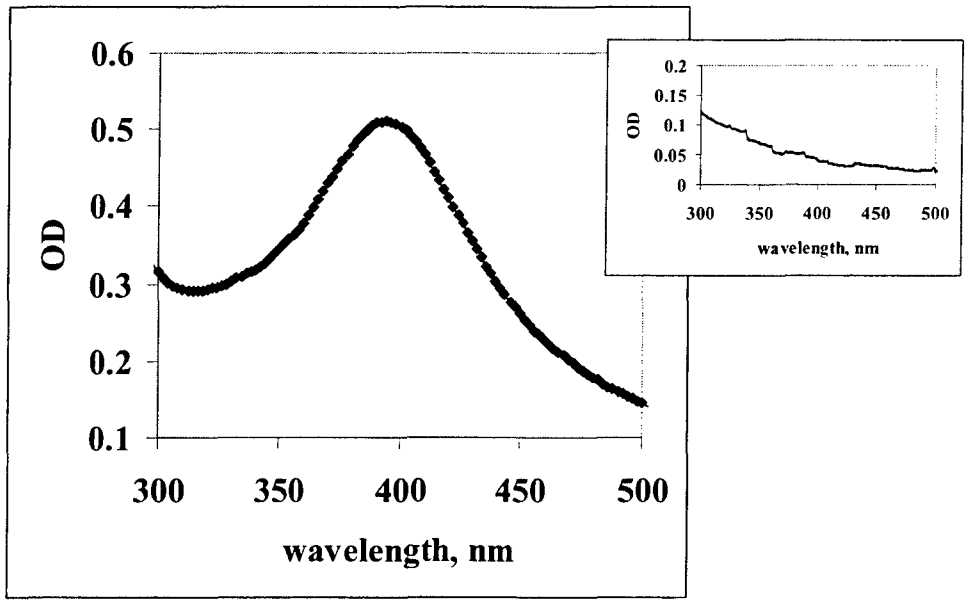

Figure 14. UV- visible absorption spectrum of suspension of *E. coli* cells with Internal Colloid (non filtered). Inset is spectrum of filtrate passed thru a 0.22 μm filter which excludes the bacteria.

When we use the reverse procedure and produce silver-coated bacteria there is a tendency for colloidal particles to cluster and precipitate out of suspension. When shaken vigorously the suspension appears gray indicating that larger, highly scattering particles are resuspended. The filtrate usually shows no appreciable signal in the UV and visible ranges, at all. Infrequently we find a few samples that have colored filtrates, with a spectrum characteristic of slightly aggregated silver colloids (as in ref. 1). This is the behavior expected of the aggregated silver coating on the micron-size bacteria, where, at times, pieces of the deposits can break loose and pass into the ambient suspension. We believe that hardly any colloid is formed directly in solution, as the reductant is initially confined to the bacteria themselves and their immediate surrounding. The cell-wall would provide efficient nucleating centers for colloid formation.

A similar behavior was exhibited during our experiments with *B. megaterrium*. The internal colloid again yields a typical colloidal spectrum, as shown in Figure 15. The wall-coated bacteria, as with *E. coli*, exhibit only a featureless extinction. A spectrum for wall-coated *E. coli* is shown in Figure 16.

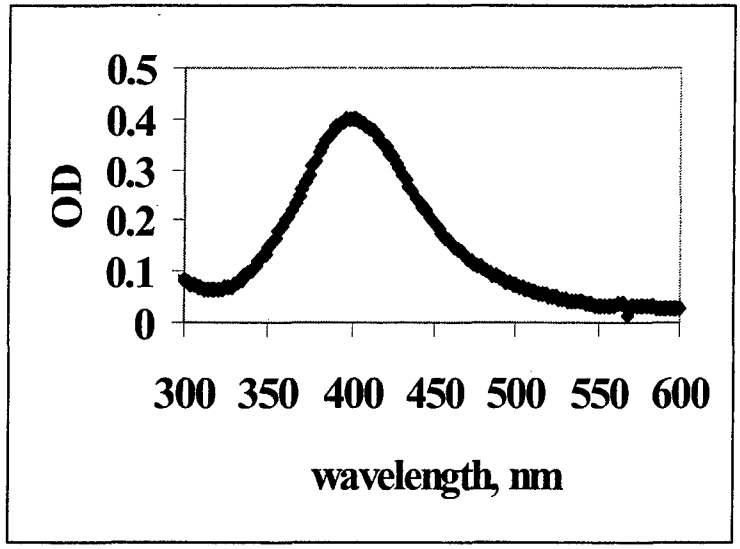

Figure 15. UV vis. absorption of a suspension of *B. meg* cells, after direct protocol showing spectrum of an internal silver colloid.

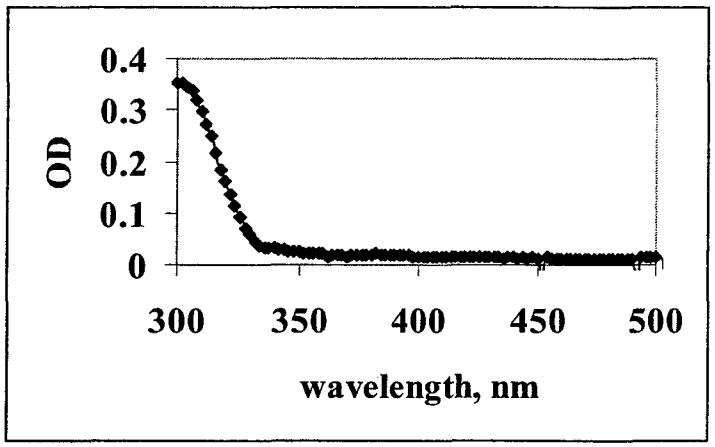

Figure 16. UV-vis absorption of a suspension of *E. coli* cells after the reverse protocol produced wall coated cells.

To further demonstrate that the presence and integrity of bacterial particles affects the production of the colloid, we used a suspension of yeast extract only (~0.1% in distilled water). Treatment with silver ions and reducing agent closely followed that for the internal colloid with bacteria. Treatment with a high concentration, 0.05N $AgNO_3$ solution (which is used with the bacteria) invariably gave a black deposit that immediately precipitated out of solution. Only diluting the silver salt down to 0.001M or below allowed production of a typical colloidal suspension resembling that obtained in the bacteria. In this case the filtered suspension gave essentially the same absorption spectrum (shown in Figure 17) as the nonfiltered one, except for a slightly lower intensity (~10%). This showed that the nanoparticles easily passed through the

0.2μm membrane filter. Dried precipitate from this suspension gave a rich SERS spectrum which was quite different from that obtained from the bacteria [Reference 2].

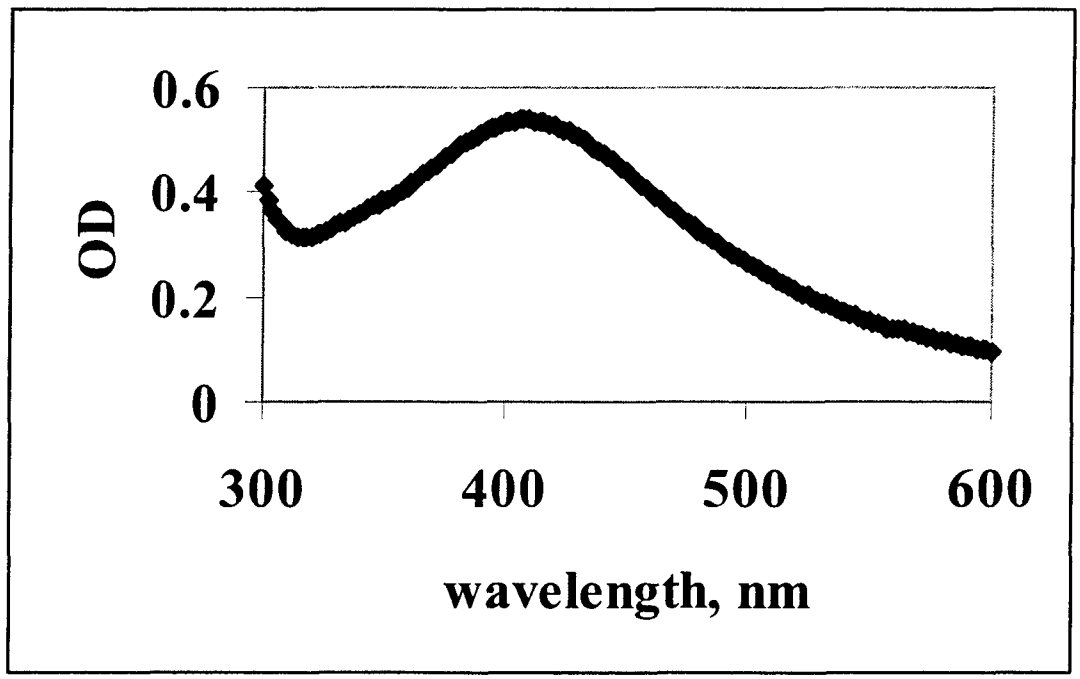

Figure 17. UV-vis absorption of a filtered colloidal suspension of silver nanoparticles obtained after treating a solution of Yeast extract with silver ions followed by reduction with sodium borohydride. Essentially the same spectrum but ~10% more intense was obtained from the unfiltered suspension.

To summarize, we find that the absorption spectra are in full agreement with the model suggesting that the bacteria provide a convenient environment for the production of silver colloids, even at high silver concentrations. The bacterial cell seems to provide a large number of efficient nucleating centers that promote the formation of nanosized particles (inside the cell) or aggregated colloidal films (on, and in, the cell surface). Local restriction of motion and limitations on the available amount of reactants also probably play a role in the processes and in the eventual stabilization of the particles.

Elemental Analysis

The results of elemental analysis of the bacteria and silver treated bacteria are summarized in Table 1 in terms of the relative molar silver/carbon ratio. In typical sample we found tens of ppm silver and 100-200 ppm carbon in our preparations except for untreated bacteria that showed negligible silver (i.e., in the sub ppm range).

TABLE 1 – Results of elemental analysis

Treatment with 0.05M Ag+	Silver/Carbon atom ratio	Estimated silver concentation, (internal colloid) or wall deposit thickness, (wall coating)*		Treatment with low Ag^+ concentrations	Silver/ carbon atom ratio	Estimated silver concentration, (internal colloid) or wall deposit thickness, (wall coating)*
Control (untreated bacteria)	$5x10^{-5}$-$3x10^{-4}$					
E. Coli, internal colloid	0.021±0.008	0.31 M		E. coli, internal colloid, 0.005M-0.0005M Ag^+	0.02±0.01	0.20 M
E. coli, wall coated	0.085±0.016	4 nm		E. coli, wall coated, 0.005M Ag^+	0.04±0.02	2.7 nm
B. meg, internal colloid	0.041±0.002	0.27 M		B. megaterium, internal colloid, 0.0005M Ag^+	0.032	0.21 M
B. meg, wall coated	0.097	2.5 nm				

Concentration and wall thickness estimates based on the above are to be discussed in a subsequent report.

Discussion and Conclusions

In this report we substantiated and extended earlier preliminary results regarding the placement of silver colloids *vis a vie* the bacteria cells. Two main modes of preparation were employed: one designed to produce the silver metal colloids within the cell (*Internal Colloid*) and the other aimed at producing a SERS active silver-coating (*Wall Coat*) of the microorganism.

TEM, UV-visible absorption, and elemental analysis consistently verified these locations of the silver within or on the cell. The internal colloid is indeed distributed uniformly thoughout the bacteria cell, while the wall deposit is concentrated at the cell surface. The intensity profile of the TEM micrographs followed the un-collapsed, cylindrical shape of the bacteria in the former case, while the micrographs of the latter showed an abrupt change of intensity at the cell wall. The intensity across a cell with a wall deposit is essentially constant and at saturation. This is in keeping with the ~2-fold higher silver content found by elemental analysis in this case compared to a cell with an internal colloid.

Wall-coated bacteria often appear to be very sticky, as evidenced by the high degree of aggregation. Cells with internal colloids are easily separated in suspension similar to controls that have no silver. Broken cells with internal colloids are seen to expel silver nanoparticles into the ambient, and correspondingly exhibit shape deformations,such as a flattening, near the rupture. They also appear lighter in the TEM micrographs particularly near the damaged areas, as expected. Silver-coated cells do not show this type of damage and release of material. It seems that a rough, although thin girdle of metallic silver holds them tightly together. The silver

coat seems to press on the cell and cause it to shrink in all dimensions. Elemental analysis reveals that silver ions tend to concentrate within (and maybe on) the bacterial cells. An enrichment by a factor of ~4-6 is observed for high ambient silver concentrations (0.05M), and the silver does not seem to wash away when the bacteria are immersed in water. Furthermore, when using a 100 fold lower concentration of the silver ions in solution, we still find the concentration within the bacteria after the direct protocol to be similar to that observed for the high ambient concentration (enrichment factor of ~600). This suggests that silver saturates sites within (and/or on) the cell with a high affinity, already at relatively low concentrations (but that are still well above the toxicity level of silver ions in cells). Using an even lower concentration of silver ions (below 5ppm, which is near the toxicity level) does behave differently, and does not produce observable colloids within the cell or on it.

Filtering samples through a 0.22 μm filter demonstrates that most of the silver colloids formed in either of the two protocols are strongly associated with the cells, and are filtered out together with the bacteria. Exceptions to this are seen from time to time with internal colloids, when damaged cells release colloids into solution

The UV-visible spectra show that the particles of the internal colloids are small and separate from each other, while the wall deposit consists of aggregated silver. Yeast extract solutions allow production of silver colloids, but only at 50 to 100 fold lower silver ion concentrations than those permitted when using bacteria. Thus, the importance of the organization of the biological material in a cellular structure is highlighted. It is not enough to have biochemicals around, for the production of stable silver colloids at high silver ion concentrations.

The dissolution of the silver (with cyanide treatment) establishes the reversibility of the process with respect to the colloids, and the fact that the silver treatment is to some extent structurally non-destructive (although the bacteria are certainly killed by the high levels of toxic silver ions).

Similar behavior is observed for *E. coli* and *B. meg* bacteria, demonstrating the generality of these findings.

We have used throughout simple physical models to allow for at least a semi-quantitative analysis of the experimental results. These models yielded values for various system variables (size, concentration, etc), which were mutually consistent, as well as reasonable.

In summary, we presented here a study of silver colloids produced and associated with two very different bacterial species, by three independent methods. The results are important in order to understand the Raman spectra we observe from these systems, as well as for the understanding of various other important phenomena, such as accumulation of minerals by bacteria, toxicity of metals, biomineralization, to mention just a few. We have also established here new ways and combinations of techniques to study such systems.

References:

1. S. Efrima, and B. V. Bronk, "Silver colloids impregnating or coating bacteria", J. Phys. Chem. vol 102, 5947-5950 (1998).

2 . S. Efrima, B. Bronk and J. Czege, "Surface enhanced Raman spectroscopy of bacteria coated with silver", Proceedings of SPIE Vol. 3533, Air Monitoring and Detection of Chemical and Biological Agents, J. Leonelli and M. L. Althouse, Editors, (1999).

3. L. Zeiri, B. V. Bronk, Y. Shabtai, J. Czégé, and S. Efrima, Silver Metal Induced Surface Enhanced Raman of Bacteria, Colloids and Surfaces A, (to be published, 2002).

4. T. Klaus, R. Joerger, E. Olsson, C. –G. Granqvist, "Silver-based crystalline nanoparticles microbially fabricated", PNAS **96,** 13611-13614 (1999).

5. R. Joerger, T. Klaus, C. –G Granqvist, "Biologically Produced Silver-Carbon Composite Materials for Optically Functional Thin-Film Coatings", Adv. Mater. **12,** 407-409 (2000).

6. T. Klaus Joerger, R. Joerger, E. Olsson, C. –G. Granqvist, "Bacteria as workers in the living factory: metal-accumulating bacteria and their potential for materials science", Trends Biotech **19**, 15-20 (2001).

7. R. C. Charley and A. T. Bull, "Bioaccumulation of silver by a multispecies community of bacteria", Arch. Microbiol. **123**, 239-244 (1979),

8. P. A. Goddard, A. T. Bull, "Accumulation of silver by growing and non-growing populations of *Citrobacter intermedius* B6", Appl. Microbiol. Biotechnol. **31**, 314-319, (1989).

9. R. M. Slawson, J. T. Trevors, H. Lee, "Silver accumulation and resistance in *Pseudomons stutzeri*" Arch. Microbiol. **158**, 398-404, (1992).

10. J. D. Holmes, P. R. Smith, R. Evans-Gowing, D. J. Richardson, D. A. Russell, J. R. Sodeau, "Bacterial photoprotection through extracellular cadmium sulfide crystallites" Photochem. Photobiol **62** , 1022-1026, (1995).

11. . Bronk, B. V., S. D. Druger, J. Czégé, W. P. Van De Merwe, "Measuring diameters of rod-shaped bacteria in vivo with polarized light", *Biophys. J.* **69:** 1170-1177 (1995).

12. G. Somorjai, in "Chemistry in Two Dimensions: Surfaces", Cornell University Press, Ithaca, p. 40 (1981).